

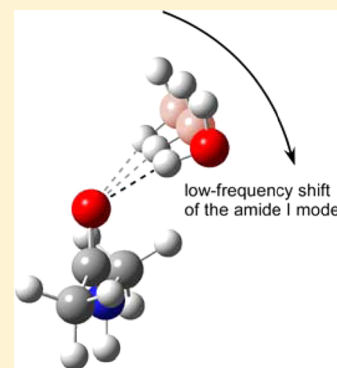
## Amide I Vibrational Properties Affected by Hydrogen Bonding Out-of-Plane of the Peptide Group

Hajime Torii\*

Department of Chemistry, Faculty of Education, and Department of Optoelectronics and Nanostructure Science, Graduate School of Science and Technology, Shizuoka University, 836 Ohya, Shizuoka 422-8529, Japan

## S Supporting Information

**ABSTRACT:** The amide I vibrational properties of a peptide–water complex in various intermolecular configurations are analyzed theoretically to see whether a water molecule with a weak out-of-plane hydrogen bond really induces a large low-frequency shift. It is shown that the frequency shift strongly depends on the  $\text{C}=\text{O}\cdots\text{H}$  angle, with a larger low-frequency shift as the  $\text{C}=\text{O}\cdots\text{H}$  becomes more bent, suggesting that the so-called hydrated helix with a rather low amide I frequency has an additional water molecule located out-of-plane of the peptide group as compared with a typical  $\alpha$ -helix. The infrared intensity also depends on the angular position of water. A new model parameter set (that can be combined with molecular dynamics) is developed for a more correct representation of the hydration-induced frequency shift. The question regarding the scalar and vectorial nature of the molecular properties related to the frequency shift is also discussed.



The amide I band is regarded as a useful marker of the secondary structures and the electrostatic situations of the peptide groups in polypeptides and proteins.<sup>1–8</sup> The vibrational properties of this mode (including the effects of neighboring peptide groups and solvent molecules) have been extensively studied from both experimental and theoretical viewpoints,<sup>9–32</sup> clarifying many aspects of those properties to the extent that we can perform linear and nonlinear spectral simulations including the effects of the dynamics in solutions.<sup>25–32</sup> However, there still remain some important points yet to be clarified. One of them would be the structural properties of the so-called hydrated helix, appearing at  $\sim 20\text{ cm}^{-1}$  lower than a typical  $\alpha$ -helix in the amide I spectral region.<sup>8,33–36</sup> In fact, this low-frequency shift is not so trivial because the peptide groups in  $\alpha$ -helices already have intrachain hydrogen bonds, so that the water molecules around those peptide groups are expected to form only weak hydrogen bonds from the side (out-of-plane of each peptide group) and/or induce partial breaking of the intrachain hydrogen bonds. This situation gives rise to the question as to whether a water molecule with a weak (less stable) out-of-plane hydrogen bond really induces a large low-frequency shift of the amide I mode. This question is also important more generally for peptide groups in proteins in aqueous solutions, where water molecules are expected to be located at various angular positions around peptide groups because of steric congestions and/or thermal fluctuations.

In spectral simulations of the amide I band, the hydration-induced frequency shift is treated theoretically based on the electrostatic mechanism, where the frequency shift is expressed as a function (called “map”) of the electrostatic potentials or electric fields at some interaction points in the peptide group. Many sets of parameters have been proposed up to now,<sup>19–27</sup>

and the differences among them are not at all subtle. With regard to this, there are two important points to note. One is the treatment of the carbonyl oxygen atom. The electrostatic situation of this atom is assumed to be totally unrelated to the amide I frequency shift in a recent parametrization (called S2),<sup>25</sup> despite the fact that this atom accepts hydrogen bonds from solvent water molecules, while it is suggested as the most important in another recent study.<sup>27</sup> The other point is that there is a discussion on whether the electrostatic potential or the electric field is the most important (or, in principle, most legitimate) quantity for the map.<sup>37</sup> In the maps developed up to now, either the electrostatic potential or electric field (but not both) is adopted as the quantity representing the electrostatic situation, and there is a discussion that the spatially nonuniform electrostatic potential cannot be ultimately ignored,<sup>37</sup> but there is no evidence that the electrostatic potentials on the atomic sites (even if sometimes supplemented by the bond centers) are sufficient for correct representation of the electrostatic situation of the peptide group in relation to its amide I frequency shift.

To solve these problems, theoretical analyses are carried out in the present study for the amide I vibrational properties of the peptide group hydrogen bonded with a water molecule at various angular positions. The *N*-methylacetamide- $d_1\cdots\text{H}_2\text{O}$  1:1 complex is selected as the model system (so that the mode may be more exactly denoted as amide I'). With regard to the hydration-induced frequency shifts of the amide I mode, a widely accepted understanding is that the effects of individual water molecules are nearly additive, as supported by the results

Received: January 2, 2015

Accepted: February 5, 2015

Published: February 5, 2015

of the previous theoretical calculations on the *N*-methylacetamide...*n*H<sub>2</sub>O (*n* = 1–3) complexes,<sup>38,39</sup> and this forms a basis of all of the electrostatic models.<sup>19–27</sup> Therefore, it is meaningful to analyze the effect of an individual water molecule on the amide I frequency shift for examining such an additive element, and it is required for any reasonable electrostatic model to reproduce the situation of the hydration of a single water molecule. The vibrational properties were calculated after optimizing the structure with the C=O...H angle (equal to 180° –  $\theta$  defined below) and the N–C=O...H dihedral angle ( $\varphi$ ) being fixed at various sets of values in the range of 0 ≤  $\theta$  ≤ 90° and 0 ≤  $\varphi$  ≤ 180° (see also Figure S1 in the Supporting Information), with density functional theory (DFT) at the B3LYP/6-31+G(2df,p) level by using the Gaussian 03 program.<sup>40</sup> The electrostatic potentials, electric fields, and field gradients at various positions were evaluated also at this level by treating the *N*-methylacetamide-*d*<sub>1</sub> molecule as a set of ghost atoms. The analyses after those calculations were carried out with our original programs. The details of the computational procedure are described in the Supporting Information.

The dependence of the vibrational frequency and infrared (IR) intensity of the amide I mode on the angular position of the hydrogen-bond-donating hydrogen atom of the water molecule is shown as two-dimensional (2D) contour plots in Figure 1. Here, the polar coordinate system ( $r$ ,  $\theta$ ,  $\varphi$ ) is defined

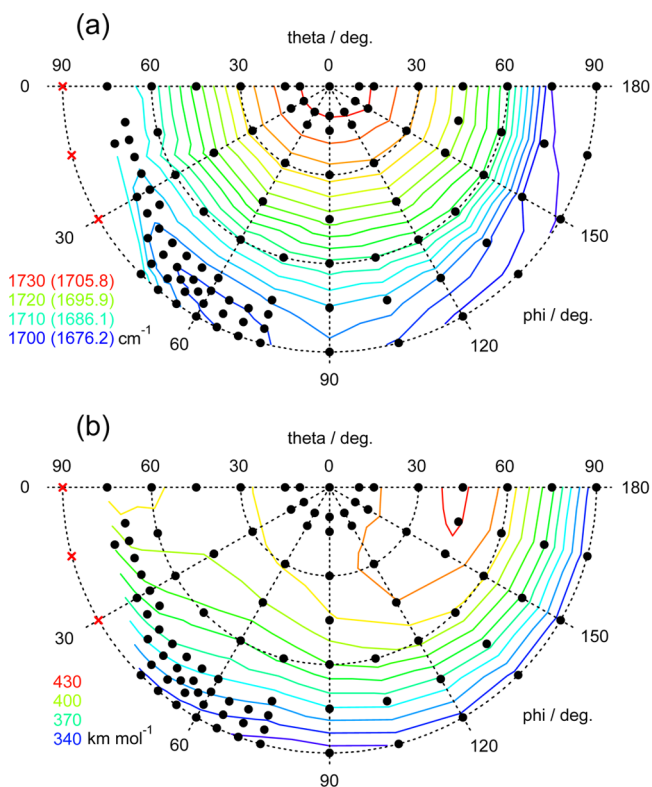


**Figure 1.** 2D contour plots of the (a) vibrational frequency and (b) IR intensity of the amide I mode calculated for the *N*-methylacetamide-*d*<sub>1</sub>...*n*H<sub>2</sub>O 1:1 complex optimized with fixed angular positions ( $\theta$  and  $\varphi$ ) of the water molecule. The calculated configurations of the complex are indicated with black filled circles. Three red  $\times$ 's indicate the angular positions where hydrogen-bonded optimized structures could not be obtained. The contours are drawn with the interval of 2 cm<sup>−1</sup> (for a) and 10 km mol<sup>−1</sup> (for b), with the color code shown on the left-hand side. The values in parentheses in part (a) are the scaled (by 0.9860) frequencies.

by taking the carbonyl oxygen atom as the origin, the C → O direction as the  $z$  axis, and the N–C=O...H dihedral angle as  $\varphi$ . It is seen that the frequency is highest at  $\theta \cong 0^\circ$  (linear C=O...H) and shifts significantly to the low-frequency side as  $\theta$  increases but does not depend much on the  $\varphi$  angle, indicating that the frequency shift is mainly related to the axially symmetric properties of the C=O bond. As shown in Figure 2a, the frequency shift is well correlated to the C=O bond length. This is consistent with the idea that the peptide–water interaction modulates the C=O bond length, and the amide I frequency shift occurs mainly because of the vibrational (mechanical) anharmonicity.<sup>23,37,41</sup> However, as shown in Figure 2c and d, the C=O bond length (and hence the frequency shift) is not well correlated to the O...H distance, which is considered to be a good indicator of the hydrogen-bond strength. (see also Figure S2 in the Supporting Information.) The present result suggests that a weak peptide–water hydrogen bond (with a long O...H distance) sometimes induces a rather large low-frequency shift of the amide I mode, giving us an idea that the so-called hydrated helix with a rather low amide I frequency may have an additional water molecule on the side (out-of-plane) of the peptide group as compared with a typical  $\alpha$ -helix in aqueous solution. Calculations on the alanine hexapeptide [CH<sub>3</sub>CO-(ala)<sub>5</sub>NHCH<sub>3</sub>] suggest that, for a deformed  $\alpha$ -helix with  $-72 \leq \Phi \leq -62^\circ$  and  $-47 \leq \Psi \leq -37^\circ$  of the backbone dihedral angles, there is room to accommodate an additional water molecule at around ( $\theta$ ,  $\varphi$ )  $\cong$  (75°, 70°) as compared with a typical  $\alpha$ -helix ( $\Phi = -57^\circ$  and  $\Psi = -47^\circ$ ). (See also Figure S3 in the Supporting Information.)

The 2D contour plot shown in Figure 1b indicates that the IR intensity is strongest at ( $\theta$ ,  $\varphi$ )  $\cong$  (45°, 180°) and is reduced as the angular position of water becomes more different from it. It is seen that the IR intensity is weakly correlated with the O...H distance, as shown in Figure 2e (rather than with the C=O bond length as shown in Figure 2b), and there is essentially no IR intensity enhancement for the complexes with longer O...H distances. However, even for those complexes, the magnitude of the induced dipole derivative [ $\delta(\partial\mu/\partial Q_{\text{aml}})$ ], defined as  $\delta(\partial\mu/\partial Q_{\text{aml}}) \equiv (\partial\mu/\partial Q_{\text{aml}})_{\text{complex}} - (\partial\mu/\partial Q_{\text{aml}})_{\text{isolated}}$ , where  $Q_{\text{aml}}$  denotes the amide I vibrational coordinate] is significantly nonzero, as shown in Figure 2f, indicating that the angle between  $\delta(\partial\mu/\partial Q_{\text{aml}})$  and  $(\partial\mu/\partial Q_{\text{aml}})_{\text{isolated}}$  is important for the IR intensity enhancement. That is, even if  $\delta(\partial\mu/\partial Q_{\text{aml}})$  is significantly nonzero, the IR intensity (proportional to  $[(\partial\mu/\partial Q_{\text{aml}})_{\text{complex}}]^2$ ) is not much enhanced if  $\delta(\partial\mu/\partial Q_{\text{aml}})$  is not sufficiently close to parallel to  $(\partial\mu/\partial Q_{\text{aml}})_{\text{isolated}}$ . In this respect, the situation is similar to that encountered in the case of the amide II mode in various conformations.<sup>42</sup>

As described above, with regard to the hydration-induced frequency shift, many different maps have been proposed in previous studies.<sup>19–27</sup> It is therefore interesting to see whether the angular position dependence shown above can be correctly represented by any of those maps. The frequency shifts predicted by those maps plotted against the DFT calculated values (scaled by 0.9860) are shown in Figure 3a–n.<sup>43</sup> [The maps are classified<sup>32</sup> here as *nPmFkG*, where P, F, and G denote the electrostatic potential, electric field, and field gradient, and *n*, *m*, and *k* represent the number of interaction points (not the number of elements).] It is seen that the predicted frequency changes are generally too small for all *nP* maps based on electrostatic potentials on atomic sites (Figure 3a–h), although the frequency shifts for typical in-plane

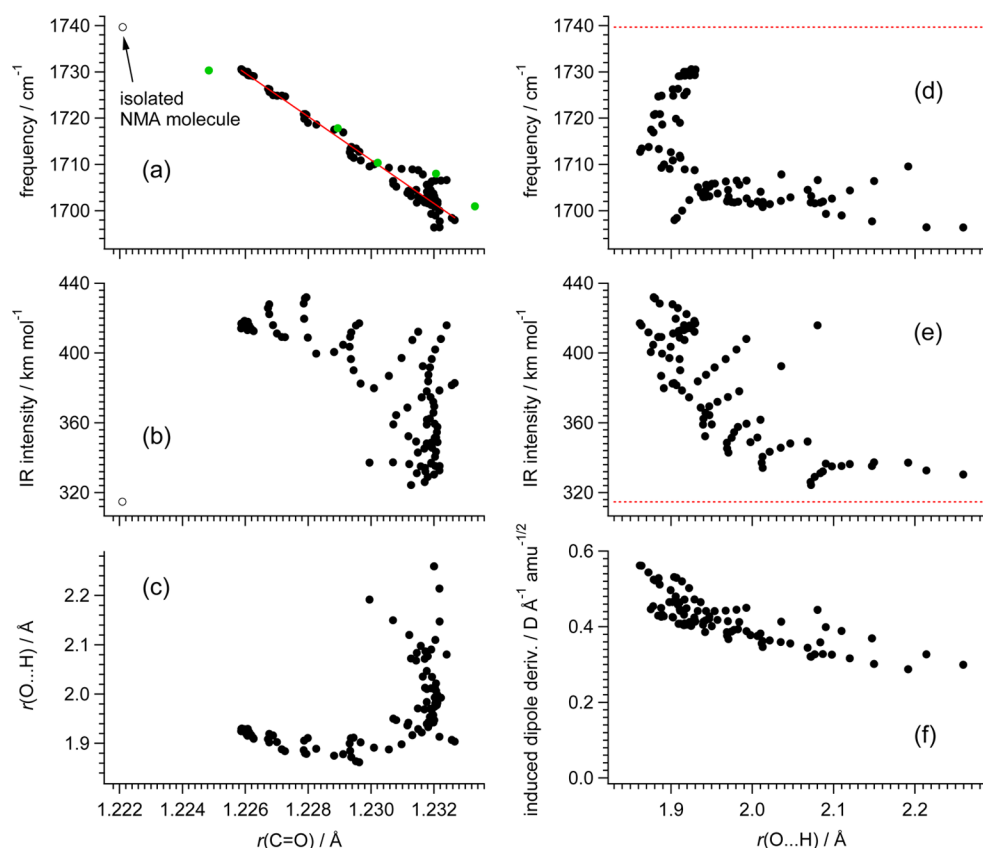


**Figure 2.** (a) Vibrational frequency and (b) IR intensity of the amide I mode, and (c) the O...H distance plotted against the C=O bond length, and (d) the vibrational frequency, (e) the IR intensity, and (f) the magnitude of the induced dipole derivative  $\delta(\partial\mu/\partial Q_{\text{aml}})$  of the amide I mode plotted against the O...H distance, calculated for the *N*-methylacetamide- $d_1$ ... $^2\text{H}_2\text{O}$  1:1 complex optimized with fixed angular positions ( $\theta$  and  $\varphi$ ) of the water molecule (shown with black filled circles). The red solid line in part (a) shows the result of the linear regression. The open circles in parts (a) and (b) and the red dotted line in parts (d) and (e) indicate the values calculated for an isolated *N*-methylacetamide- $d_1$  molecule.<sup>39</sup> The green filled circles shown in part (a) indicate the values calculated for some fully optimized structures of the *N*-methylacetamide- $d_1$ ... $n^2\text{H}_2\text{O}$  complexes ( $n = 1$  and 2),<sup>39</sup> showing that the correlation between the frequency and the C=O bond length is essentially the same.

hydrogen-bonding configurations [ $(\theta, \varphi) = (45^\circ, 0^\circ)$  and  $(60^\circ, 180^\circ)$ , marked with black bold X's] are successfully reproduced by those maps. As shown in Figure 2d, complexes with similar O...H distances (of  $\sim 1.9$  Å) have significantly different amide I frequencies depending on the angular positions of hydration water, but the carbonyl oxygen atom feels a similar electrostatic potential in complexes with similar O...H distances, resulting in similar predicted values. Comparing the results obtained for the 1F maps (Figure 3m and n),<sup>23,27</sup> it is clear that the location of the interaction point [ $x = 1.0$  and  $0.23$ , respectively, for  $\mathbf{r} = x\mathbf{r}_\text{O} + (1-x)\mathbf{r}_\text{C}$ ] is an important factor, indicating that the idea of locating the interaction point of the electric field only at the outermost atomic site is too simple in this case (although it works quite well for the OH stretching mode of water<sup>44–47</sup>). Among the maps proposed previously, the 4F and 2F maps shown in Figure 3j and k (called S13 and S2)<sup>24,25</sup> seem to be better than the others, but the agreement is not considered to be sufficient. Note that, in these two maps, the coefficients for the carbonyl oxygen are not large (S13) or totally zero (S2).

This situation indicates that the angular position dependence shown above is not a corollary of any of the previously developed maps. Then, how can we understand it? Discussion in some previous studies suggests that the response of molecular vibrations to the intermolecular electrostatic situation is mainly related to the dipole derivative of the mode.<sup>37,48,49</sup> Then, the problem is how we locate each element

of the dipole derivative. Here, we propose a new model (a new map) based on the idea that the dipole derivative is decomposed into the contributions of atomic nuclei, core electrons, and valence electrons. The contribution of atomic nuclei arises from the atomic displacement vector  $(\partial\mathbf{r}_n/\partial Q_{\text{aml}})$  multiplied by the electric charge ( $Z_n$ ) of each atomic nucleus (numbered by  $n$ ), which is apparently located on each atomic site. It is assumed here that the core electrons faithfully follow the atomic nuclei, so that the effective charge would be  $Z_n^{(\text{eff})} = Z_n - 2e$  for the C, O, and N atoms. It should be noted that the molecular property in charge of this part is *vectorial in nature* and cannot be represented by a model based on the electrostatic potential at a small number of interaction points. In other words, the electric field is a legitimate quantity for representing the hydration-induced frequency shift. With regard to the contribution of the valence electrons, we adopt a model that it arises from the charge flux<sup>39,50–55</sup> (represented by  $\partial q_n/\partial Q_{\text{aml}}$ , where  $q_n$  is the electric charge of atom  $n$ ) between the carbonyl C and O atoms. Then, within the one-mode harmonic approximation, the displacement  $\delta Q_{\text{aml}}$  along the amide I mode is expressed as

$$\delta Q_{\text{aml}} = \frac{1}{k_{\text{aml}}} \left( f \sum_n Z_n^{(\text{eff})} \frac{\partial \mathbf{r}_n}{\partial Q_{\text{aml}}} \cdot \mathbf{E}_n - g \sum_n \frac{\partial q_n}{\partial Q_{\text{aml}}} \Phi_n \right) \quad (1)$$

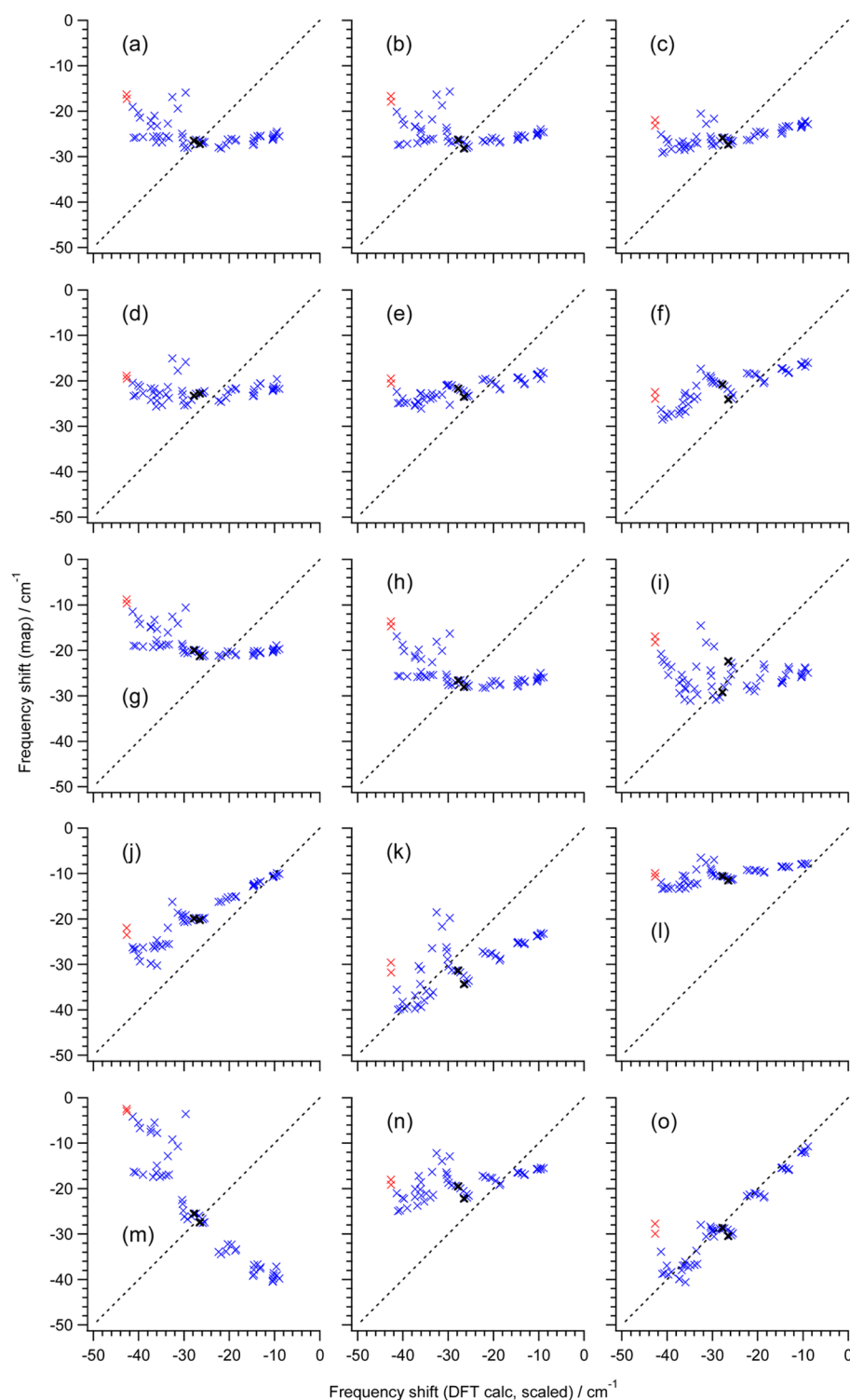


**Figure 3.** Frequency shifts of the amide I mode predicted by (a–n) the previously proposed maps [(a) Cho 4P,<sup>19</sup> (b) Cho 6P,<sup>20</sup> (c) Bouř 5P,<sup>21</sup> (d) Hirst 4P,<sup>22</sup> (e) Hirst 7P,<sup>22</sup> (f) Skinner 6P,<sup>24</sup> (g) Tokmakoff 2P,<sup>27</sup> (h) Tokmakoff 4P,<sup>27</sup> (i) Jansen 4F4G,<sup>26</sup> (j) Skinner 4F (S13),<sup>24</sup> (k) Skinner 2F (S2),<sup>25</sup> (l) Tokmakoff 2F,<sup>27</sup> (m) Tokmakoff 1F,<sup>27</sup> and (n) Torii 1F<sup>23</sup>] and (o) the new 2P3F map proposed in this study (before fine-tuning, with  $f = 0.4$  and  $g = 1.0$  in eq 1), plotted against the values directly calculated at the B3LYP/6-31+G(2df,p) level (scaled by 0.9860) for the *N*-methylacetamide- $d_1\cdots^2$ H<sub>2</sub>O 1:1 complex optimized with fixed angular positions ( $\theta$  and  $\varphi$ ) of the water molecule. The two black bold x's in each panel represent the points of typical in-plane hydrogen-bonding configurations [ $(\theta, \varphi) = (45^\circ, 0^\circ)$  and  $(60^\circ, 180^\circ)$ ], and the two red x's represent the points excluded in the fitting for developing the new map [ $(\theta, \varphi) = (90^\circ, 165^\circ)$  and  $(90^\circ, 180^\circ)$ ]. The black dotted line is the line of gradient unity passing through the origin.

where  $\Phi_n$  and  $E_n$  are the electrostatic potential and electric field at atom  $n$ ,  $k_{\text{amI}}$  is the force constant of the amide I mode (of an isolated molecule), and  $f$  and  $g$  are the scale factors of the two

terms (discussed below). (See also section 3 in the Supporting Information for the derivation.) The amide I frequency shift ( $\delta\tilde{\nu}_{\text{amI}}$ ) is calculated by using  $\partial[r(\text{C}=\text{O})]/\partial Q_{\text{amI}}$  (equal to



$0.3725 \text{ \AA}(\text{\AA} \text{ amu}^{1/2})^{-1}$ , obtained from the atomic displacements of the mode of an isolated molecule) and  $\partial[\delta\tilde{\nu}_{\text{aml}}]/\partial[r(\text{C}=\text{O})]$  (equal to  $-4603 \text{ cm}^{-1} \text{ \AA}^{-1}$ , obtained from the linear regression line shown in Figure 2a). Considering the result obtained in Figure 1, only the  $z$  component (along the  $\text{C}=\text{O}$  bond) of  $\partial r_n/\partial Q_{\text{aml}}$  is taken into account, and only the C, O, and N atomic sites in the peptide group are included in the summation in eq 1 as an approximation.

In examining the performance of this 2P3F model, it was found that the contribution of the first term is overestimated by a factor of  $\sim 2.5$ , probably because some of the valence electrons also follow the atomic nuclei. The result obtained with  $f = 0.4$  and  $g = 1.0$  is shown in Figure 3o. It is clear that the agreement is significantly improved as compared with the previous maps, except for the two points  $[(\theta, \varphi) = (90^\circ, 165^\circ)$  and  $(90^\circ, 180^\circ)]$  shown with red X's. Assuming that the occurrence of these angular positions is rather rare (because of the rather high relative energy of  $\sim 7 \times 10^{-3} E_{\text{h}}$ ), least-squares fitting was performed for the scale factors  $f$  and  $g$  by excluding these two points. The resulting coefficients of the new 2P3F map (with  $f = 0.4181$  and  $g = 0.9870$ ) expressed as

$$\delta\tilde{\nu}_{\text{aml}} = \sum_n [d_n(E_z)_n + l_n\Phi_n] \quad (2)$$

are  $d_n = 3031.6, -2751.2$ , and  $-357.9 \text{ cm}^{-1} (E_{\text{h}} a_0^{-1} e^{-1})^{-1}$  for C, O, and N and  $l_n = 2240.0$  and  $-2240.0 \text{ cm}^{-1} (E_{\text{h}} e^{-1})^{-1}$  for C and O. As shown in Figure 4a, the agreement is considered to be reasonable. This parameter set corresponds to the charge flux of  $|\partial q/\partial Q_{\text{aml}}| = 0.5420 e \text{ \AA}^{-1} \text{ amu}^{-1/2}$  and the dipole derivative of  $|\partial \mu/\partial Q_{\text{aml}}| = 3.134 \text{ D \AA}^{-1} \text{ amu}^{-1/2}$  (equivalent to the IR intensity of  $415.0 \text{ km mol}^{-1}$ ), which are also considered to be reasonable.

Having obtained this result on the angular position dependence of the frequency shift, it would be interesting to see how this new parameter set performs for reproducing the dependence of the frequency shift on the  $\text{O}\cdots\text{H}$  distance at specified angular positions. The results obtained for some representative angular positions  $[\theta \cong 0^\circ \text{ and } (\theta, \varphi) = (45^\circ, 0^\circ), (60^\circ, 90^\circ), \text{ and } (60^\circ, 180^\circ)]$  are shown in Figure 4b–e. It is clearly seen that the agreement is reasonable also in this case. We note that the angular position dependence of the frequency shift is reduced as the  $\text{O}\cdots\text{H}$  distance becomes longer (as easily recognized by comparing the values at longer  $\text{O}\cdots\text{H}$  distances in Figure 4b–e). With regard to the elements appearing in eq 1,  $\partial q_n/\partial Q_{\text{aml}}$  of each atom works isotropically around it, while  $Z_n^{(\text{eff})}(\partial r_n/\partial Q_{\text{aml}})$  is anisotropic (axially symmetric) in nature. Because the latter is mainly responsible for the angular position dependence and its effect (related to electric field) diminishes faster than that of the former (related to electrostatic potential) as the  $\text{O}\cdots\text{H}$  distance becomes longer, the reduced angular position dependence at longer  $\text{O}\cdots\text{H}$  distances is considered to be natural. We also point out that, in a usual situation of the  $\text{C}=\text{O}\cdots\text{H}$  hydrogen bond, the frequency shift arising from the electrostatic situation of the O atom [a positive  $\Phi_n$  and a negative  $(E_z)_n$  (i.e., the field in the  $\text{O} \rightarrow \text{C}$  direction)] contains significant mutual cancellation between the first and second terms in eq 2 of the present 2P3F model. This would probably be the reason why the frequency shift is concluded as less sensitive (than expected) to the electrostatic situation of the O atom in some previous<sup>24,25</sup> maps.

In summary, it has been shown that the hydration-induced frequency shift and IR intensity enhancement of the amide I mode have large dependence on the angular position of water.

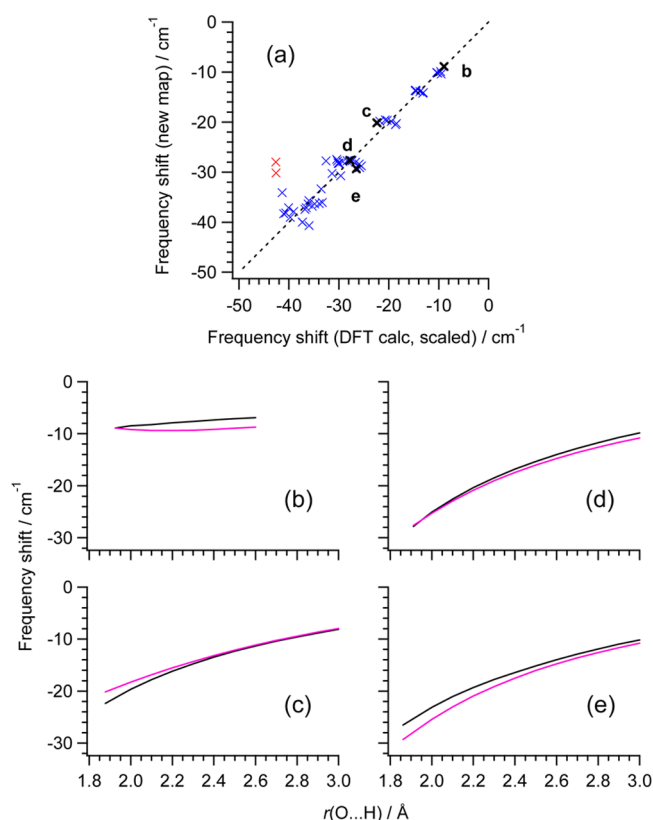


**Figure 4.** (a) Frequency shifts of the amide I mode predicted by the new 2P3F map proposed in this study (after fine-tuning, with  $f = 0.4181$  and  $g = 0.9870$  in eq 1), plotted against the values directly calculated at the B3LYP/6-31+G(2df,p) level (scaled by 0.9860) for the  $N$ -methylacetamide- $d_1\cdots^2\text{H}_2\text{O}$  1:1 complex optimized with fixed angular positions ( $\theta$  and  $\varphi$ ) of the water molecule. The four black bold X's labeled as b–e indicate the angular positions where the distance dependence is also examined. The two red X's represent the points excluded in the fitting for developing the new map  $[(\theta, \varphi) = (90^\circ, 165^\circ)$  and  $(90^\circ, 180^\circ)]$ . The black dotted line is the line of gradient unity passing through the origin. (b–e) Dependence of the amide I frequency shift on the  $\text{O}\cdots\text{H}$  distance at the angular positions of  $\theta \cong 0^\circ$  and  $(\theta, \varphi) = (45^\circ, 0^\circ), (60^\circ, 90^\circ), \text{ and } (60^\circ, 180^\circ)$ , respectively (marked with black bold X's in part a). Pink solid line: predicted by the new 2P3F map; black solid line: directly calculated at the B3LYP/6-31+G(2df,p) level (scaled by 0.9860).

A larger frequency shift is induced as the  $\theta$  angle (defined as  $180^\circ$  minus the  $\text{C}=\text{O}\cdots\text{H}$  angle) becomes larger. This result suggests that the so-called hydrated helix with a rather low amide I frequency may have an additional water molecule on the side (out of plane) of the peptide group as compared with a typical  $\alpha$ -helix. A new 2P3F map (describing the frequency shift as a function of the electrostatic situation of the peptide group) has been developed to reproduce this angular position dependence, clarifying that (1) part of the molecular properties describing the vibrational response to the electrostatic situation should be vectorial in nature and (2) the electrostatic situation of the carbonyl oxygen atom is not at all negligible but the scalar and vectorial elements on it contribute destructively for the hydration-induced frequency shift of the amide I mode. Having obtained this new map, it is expected that we can do improved spectral simulations of proteins in aqueous solutions. This point will be examined in future studies.

## ■ ASSOCIATED CONTENT

## ■ Supporting Information

The details of the computational procedures are described. The figure of the polar coordinate system ( $\theta$  and  $\varphi$ ), the figure of the relation between the relative potential energy (indicating the hydrogen-bond strength) and the O...H distance and the table of the structural and vibrational properties of the calculated *N*-methylacetamide- $d_1\cdots^2\text{H}_2\text{O}$  1:1 complexes, and the figure of the locations of water molecules hydrogen-bonded to a peptide chain in a deformed  $\alpha$ -helix conformation are shown. This material is available free of charge via the Internet at <http://pubs.acs.org>.

## ■ AUTHOR INFORMATION

## Corresponding Author

\*E-mail: [torii.hajime@shizuoka.ac.jp](mailto:torii.hajime@shizuoka.ac.jp). Telephone and Fax: +81-54-238-4624

## Notes

The authors declare no competing financial interest.

## ■ ACKNOWLEDGMENTS

This study was supported in part by a Grant-in-Aid for Scientific Research from the Ministry of Education, Culture, Sports, Science, and Technology.

## ■ REFERENCES

- (1) Byler, D. M.; Susi, H. Examination of the Secondary Structure of Proteins by Deconvolved FTIR Spectra. *Biopolymers* **1986**, *25*, 469–487.
- (2) Miyazawa, T. Perturbation Treatment of the Characteristic Vibrations of Polypeptide Chains in Various Configurations. *J. Chem. Phys.* **1960**, *32*, 1647–1652.
- (3) Miyazawa, T.; Blout, E. R. The Infrared Spectra of Polypeptides in Various Conformations: Amide I and II Bands. *J. Am. Chem. Soc.* **1961**, *83*, 712–719.
- (4) Krimm, S.; Bandekar, J. Vibrational Spectroscopy and Conformation of Peptides, Polypeptides, and Proteins. *Adv. Protein Chem.* **1986**, *38*, 181–364.
- (5) Mantsch, H. H.; Casal, H. L.; Jones, R. N. Resolution Enhancement of Infrared Spectra of Biological Systems. In *Spectroscopy of Biological Systems*, Advances in Spectroscopy; Clark, R. J. H., Hester, R. E., Eds.; Wiley: New York, 1986; Vol. 13, pp 1–46.
- (6) Surewicz, W. K.; Mantsch, H. H.; Chapman, D. Determination of Protein Secondary Structure by Fourier Transform Infrared Spectroscopy: A Critical Assessment. *Biochemistry* **1993**, *32*, 389–394.
- (7) Torii, H.; Tasumi, M. Theoretical Analyses of the Amide I Infrared Bands of Globular Proteins. In *Infrared Spectroscopy of Biomolecules*; Mantsch, H. H., Chapman, D., Eds.; Wiley-Liss: New York, 1996; pp 1–18.
- (8) Barth, A. Infrared Spectroscopy of Proteins. *Biochim. Biophys. Acta* **2007**, *1767*, 1073–1101.
- (9) Schweitzer-Stenner, R. Visible and UV-Resonance Raman Spectroscopy of Model Peptides. *J. Raman Spectrosc.* **2001**, *32*, 711–732.
- (10) Brauner, J. W.; Flach, C. R.; Mendelsohn, R. A Quantitative Reconstruction of the Amide I Contour in the IR Spectra of Globular Proteins: From Structure to Spectrum. *J. Am. Chem. Soc.* **2005**, *127*, 100–109.
- (11) Chen, X. G.; Schweitzer-Stenner, R.; Krimm, S.; Mirkin, N. G.; Asher, S. A. *N*-Methylacetamide and Its Hydrogen-Bonded Water Molecules Are Vibrationally Coupled. *J. Am. Chem. Soc.* **1994**, *116*, 11141–11142.
- (12) Hamm, P.; Lim, M.; DeGrado, W. F.; Hochstrasser, R. M. The Two-Dimensional IR Nonlinear Spectroscopy of a Cyclic Penta-Peptide in Relation to Its Three-Dimensional Structure. *Proc. Natl. Acad. Sci. U.S.A.* **1999**, *96*, 2036–2041.
- (13) Chung, H. S.; Khalil, M.; Tokmakoff, A. Nonlinear Infrared Spectroscopy of Protein Conformational Change during Thermal Unfolding. *J. Phys. Chem. B* **2004**, *108*, 15332–15342.
- (14) Krimm, S.; Abe, Y. Intermolecular Interaction Effects in the Amide I Vibrations of  $\beta$  Polypeptides. *Proc. Natl. Acad. Sci. U.S.A.* **1972**, *69*, 2788–2792.
- (15) Torii, H.; Tasumi, M. Model Calculations on the Amide-I Infrared Bands of Globular Proteins. *J. Chem. Phys.* **1992**, *96*, 3379–3387.
- (16) Torii, H.; Tasumi, M. *Ab Initio* Molecular Orbital Study of the Amide I Vibrational Interactions between the Peptide Groups in Di- and Tripeptides and Considerations on the Conformation of the Extended Helix. *J. Raman Spectrosc.* **1998**, *29*, 81–86.
- (17) Hamm, P.; Woutersen, S. Coupling of the Amide I Modes of the Glycine Dipeptide. *Bull. Chem. Soc. Jpn.* **2002**, *75*, 985–988.
- (18) Gorbunov, R. D.; Kosov, D. S.; Stock, G. *Ab Initio*-Based Exciton Model of Amide I Vibrations in Peptides: Definition, Conformational Dependence, and Transferability. *J. Chem. Phys.* **2005**, *122*, 224904.
- (19) Ham, S.; Cho, M. Amide I Modes in the *N*-Methylacetamide Dimer and Glycine Dipeptide Analog: Diagonal Force Constants. *J. Chem. Phys.* **2003**, *118*, 6915–6922.
- (20) Kwac, K.; Cho, M. Molecular Dynamics Simulation Study of *N*-Methylacetamide in Water. I. Amide I Mode Frequency Fluctuation. *J. Chem. Phys.* **2003**, *119*, 2247–2255.
- (21) Bouř, P.; Keiderling, T. A. Empirical Modeling of the Peptide Amide I Band IR Intensity in Water Solution. *J. Chem. Phys.* **2003**, *119*, 11253–11262.
- (22) Watson, T. M.; Hirst, J. D. Theoretical Studies of the Amide I Vibrational Frequencies of [Leu]-Enkephalin. *Mol. Phys.* **2005**, *103*, 1531–1546.
- (23) Torii, H. Electrostatic Origin of the Cooperative Effect on the C=O Bond Lengths and the Amide I Vibrational Frequencies of the *N*-Methylacetamide Oligomers. *J. Mol. Struct.* **2005**, *735/736*, 21–26.
- (24) Schmidt, J. R.; Corcelli, S. A.; Skinner, J. L. Ultrafast Vibrational Spectroscopy of Water and Aqueous *N*-Methylacetamide: Comparison of Different Electronic Structure/Molecular Dynamics Approaches. *J. Chem. Phys.* **2004**, *121*, 8887–8896.
- (25) Wang, L.; Middleton, C. T.; Zanni, M. T.; Skinner, J. L. Development and Validation of Transferable Amide I Vibrational Frequency Maps for Peptides. *J. Phys. Chem. B* **2011**, *115*, 3713–3724.
- (26) Jansen, T. I. C.; Knoester, J. A Transferable Electrostatic Map for Solvation Effects on Amide I Vibrations and its Application to Linear and Two-Dimensional Spectroscopy. *J. Chem. Phys.* **2006**, *124*, 044502.
- (27) Reppert, M.; Tokmakoff, A. Electrostatic Frequency Shifts in Amide I Vibrational Spectra: Direct Parameterization against Experiment. *J. Chem. Phys.* **2013**, *138*, 134116.
- (28) Moran, A. M.; Park, S.-M.; Mukamel, S. Infrared Photon Echo Signatures of Hydrogen Bond Connectivity in the Cyclic Dipeptide Antamanide. *J. Chem. Phys.* **2003**, *118*, 9971–9980.
- (29) Maekawa, H.; Ballano, G.; Toniolo, C.; Ge, N.-H. Linear and Two-Dimensional Infrared Spectroscopic Study of the Amide I and II Modes in Fully Extended Peptide Chains. *J. Phys. Chem. B* **2011**, *115*, 5168–5182.
- (30) Torii, H. Effects of Intermolecular Vibrational Coupling and Liquid Dynamics on the Polarized Raman and Two-Dimensional Infrared Spectral Profiles of Liquid *N,N*-Dimethylformamide Analyzed with a Time-Domain Computational Method. *J. Phys. Chem. A* **2006**, *110*, 4822–4832.
- (31) Jansen, T. I. C.; Knoester, J. Nonadiabatic Effects in the Two-Dimensional Infrared Spectra of Peptides: Application to Alanine Dipeptide. *J. Phys. Chem. B* **2006**, *110*, 22910–22916.
- (32) Ganim, Z.; Tokmakoff, A. Spectral Signatures of Heterogeneous Protein Ensembles Revealed by MD Simulations of 2DIR Spectra. *Biophys. J.* **2006**, *91*, 2636–2646.
- (33) Gilmanishin, R.; Williams, S.; Callender, R. H.; Woodruff, W. H.; Dyer, R. B. Fast Events in Protein Folding: Relaxation Dynamics and

Structure of the I Form of Apomyoglobin. *Biochemistry* **1997**, *36*, 15006–15012.

(34) Reisdorf, W. C., Jr.; Krimm, S. Infrared Amide I' Band of the Coiled Coil. *Biochemistry* **1996**, *35*, 1383–1386.

(35) Manas, E. S.; Getahun, Z.; Wright, W. W.; DeGrado, W. F.; Vanderkooi, J. M. Infrared Spectra of Amide Groups in  $\alpha$ -Helical Proteins: Evidence for Hydrogen Bonding between Helices and Water. *J. Am. Chem. Soc.* **2000**, *122*, 9883–9890.

(36) Walsh, S. T. R.; Cheng, R. P.; Wright, W. W.; Alonso, D. O. V.; Daggett, V.; Vanderkooi, J. M.; DeGrado, W. F. The Hydration of Amides in Helices; A Comprehensive Picture from Molecular Dynamics, IR, and NMR. *Protein Sci.* **2003**, *12*, 520–531.

(37) Cho, M. Vibrational Solvatochromism and Electrochromism: Coarse-Grained Models and Their Relationships. *J. Chem. Phys.* **2009**, *130*, 094505.

(38) Torii, H.; Tatsumi, T.; Tasumi, M. Effects of Hydration on the Structure, Vibrational Wavenumbers, Vibrational Force Field, and Resonance Raman Intensities of *N*-Methylacetamide. *J. Raman Spectrosc.* **1998**, *29*, 537–546.

(39) Torii, H. Intermolecular Charge Flux as the Origin of Infrared Intensity Enhancement upon Halogen-Bond Formation of the Peptide Group. *J. Chem. Phys.* **2010**, *133*, 034504.

(40) Frisch, M. J.; Trucks, G. W.; Schlegel, H. B.; Scuseria, G. E.; Robb, M. A.; Cheeseman, J. R.; Montgomery, J. A., Jr.; Vreven, T.; Kudin, K. N.; Burant, J. C.; et al. *Gaussian 03*, revision D.01; Gaussian, Inc.: Wallingford, CT, 2004.

(41) Torii, H. Vibrational Interactions in the Amide I Subspace of the Oligomers and Hydration Clusters of *N*-Methylacetamide. *J. Phys. Chem. A* **2004**, *108*, 7272–7280.

(42) Torii, H. Mechanism of the Secondary Structure Dependence of the Infrared Intensity of the Amide II Mode of Peptide Chains. *J. Phys. Chem. Lett.* **2012**, *3*, 112–116.

(43) Note that each of these maps has an offset frequency value to calculate absolute frequency positions. Therefore, in this comparison, an emphasis should be laid on the gradient of the principal axis of the correlation (whether it is close to unity or not) rather than the absolute frequency shifts.

(44) Corcelli, S. A.; Skinner, J. L. Infrared and Raman Line Shapes of Dilute HOD in Liquid H<sub>2</sub>O and D<sub>2</sub>O from 10 to 90 °C. *J. Phys. Chem. A* **2005**, *109*, 6154–6165.

(45) Schmidt, J. R.; Corcelli, S. A.; Skinner, J. L. Pronounced Non-Condon Effects in the Ultrafast Infrared Spectroscopy of Water. *J. Chem. Phys.* **2005**, *123*, 044513.

(46) Torii, H. Time-Domain Calculations of the Polarized Raman Spectra, the Transient Infrared Absorption Anisotropy, and the Extent of Delocalization of the OH Stretching Mode of Liquid Water. *J. Phys. Chem. A* **2006**, *110*, 9469–9477.

(47) Torii, H. Intra- and Intermolecular Charge Fluxes Induced by the OH Stretching Mode of Water and Their Effects on the Infrared Intensities and Intermolecular Vibrational Coupling. *J. Phys. Chem. B* **2010**, *114*, 13403–13409.

(48) Torii, H. The Role of Electrical Property Derivatives in Intermolecular Vibrational Interactions and Their Effects on Vibrational Spectra. *Vib. Spectrosc.* **2002**, *29*, 205–209.

(49) Torii, H. Responses of Molecular Vibrations to Intermolecular Electrostatic Interactions and Their Effects on Vibrational Spectroscopic Features. In *Atoms, Molecules and Clusters in Electric Fields. Theoretical Approaches to the Calculation of Electric Polarizability*; Maroulis, G., Ed.; Imperial College Press: London, 2006; pp 179–214.

(50) Decius, J. C. An Effective Atomic Charge Model for Infrared Intensities. *J. Mol. Spectrosc.* **1975**, *57*, 348–362.

(51) van Straten, A. J.; Smit, W. M. A. Bond Charge Parameters from Integrated Infrared Intensities. *J. Mol. Spectrosc.* **1976**, *62*, 297–312.

(52) Gussoni, M.; Castiglioni, C.; Zerbi, G. Physical Meaning of Electrooptical Parameters Derived from Infrared Intensities. *J. Phys. Chem.* **1984**, *88*, 600–604.

(53) Torii, H.; Tasumi, M. Infrared Intensities of Vibrational Modes of an  $\alpha$ -Helical Polypeptide: Calculations Based on the Equilibrium

Charge/Charge Flux (ECCF) Model. *J. Mol. Struct.* **1993**, *300*, 171–179.

(54) Palmo, K.; Mannfors, B.; Mirkin, N. G.; Krimm, S. Potential Energy Functions: From Consistent Force Fields to Spectroscopically Determined Polarizable Force Fields. *Biopolymers* **2003**, *68*, 383–394.

(55) Torii, H. Delocalized Electrons in Infrared Intensities. *J. Mol. Struct.* **2014**, *1056/1057*, 84–96.